

Dark-matter sterile neutrinos in models with a gauge singlet in the Higgs sector

Kalliopi Petraki and Alexander Kusenko

Department of Physics and Astronomy, University of California, Los Angeles, CA 90095-1547, USA

Sterile neutrino with mass of several keV can be the cosmological dark matter, can explain the observed velocities of pulsars, and can play an important role in the formation of the first stars. We describe the production of sterile neutrinos in a model with an extended Higgs sector, in which the Majorana mass term is generated by the expectation value of a gauge-singlet Higgs boson. In this model the relic abundance of sterile neutrinos does not necessarily depend on their mixing angles, the free-streaming length can be much smaller than in the case of warm dark matter produced by neutrino oscillations, and, therefore, some of the previously quoted bounds do not apply. The presence of the gauge singlet in the Higgs sector has important implications for the electroweak phase transition, baryogenesis, and the upcoming experiments at the Large Hadron Collider and a Linear Collider.

PACS numbers: 14.60.St, 95.35.+d,

UCLA/07/TEP/27

I. INTRODUCTION

The discovery of the neutrino masses can easily be incorporated into the Standard Model (SM) by adding two or more $SU(3) \times SU(2) \times U(1)$ singlet fermions, often called right-handed neutrinos, which are allowed to have the Yukawa couplings to the Higgs boson and the standard, left-handed neutrinos. The Yukawa couplings generate the Dirac mass terms for the neutrinos after the spontaneous symmetry breaking. In addition, the singlet fermions can have some Majorana masses. The interplay between the Dirac mass and the Majorana mass, known as the seesaw mechanism [1], can accommodate the observed neutrino masses for a variety of Majorana masses. If the Majorana mass terms are large, the particles associated with the singlet fields are very heavy. However, if one or more Majorana masses are below the electroweak scale, the so called sterile neutrinos appear among the low-energy degrees of freedom. These new particles can be the cosmological dark matter [2, 3, 4, 5, 6, 7, 8], their production in a supernova can explain the pulsar kicks [9] and can affect the supernova explosion in a variety of ways [10]; the same particles can play an important role in the formation of the first stars [11] and some other astrophysical phenomena [12].

The properties of the sterile dark matter, and, in particular, how warm or cold it is for a given mass, depend on the production mechanism. One mechanism, which generates a population of relic sterile neutrinos at the sub-GeV temperature was proposed by Dodelson and Widrow (DW) [2]. If the lepton asymmetry is negligible, this scenario appears to be in conflict with a combination of the X-ray bounds [13] and the Lyman- α bounds [14, 15]. This conclusion is based on the state-of-the-art calculations of the sterile neutrino production in neutrino oscillations [3]. It is possible to evade this constraint if the lepton asymmetry of the universe is greater than (10^{-3}) [4]. On the other hand, some astronomical observations [16, 17] point to a non-negligible free-streaming length for dark matter, which favors warm dark matter. Moreover, warm dark matter can cause filamentary

structure on small scales [18], in contrast with cold dark matter. It is also possible that the sterile neutrinos make up only a fraction of dark matter [15], in which case they can still be responsible for the observed velocities of pulsars [7, 9].

Dodelson–Widrow mechanism is not the only mechanism by which sterile dark matter could be produced. The relic population of sterile neutrinos could be generated in a variety of ways, for example, from their coupling to the inflaton [6], the electroweak-singlet Higgs boson [7], or the radion [8]. Whatever the production history of sterile neutrinos might be at the high temperature, there is always some additional amount produced in neutrino oscillations at some sub-GeV temperatures [2, 3]. The two components can have very different momentum distributions. Therefore, generically this form of dark matter is a mixed two-component dark matter, which can have some very interesting observable consequences [19].

In this paper we concentrate on the possibility that the relatively light Majorana mass could arise via the Higgs mechanism in a model with an $SU(2) \times U(1)$ -singlet Higgs boson coupled to the Standard Model Higgs boson [20], and that the sterile neutrinos could be produced from the Higgs decays at a temperature as high as 100 GeV [7]. We will explore various scenarios for such production and the implications for the electroweak phase transition. In particular, we will address the cooling and the red-shifting of dark matter, which have important implications for dark matter profiles in halos [16, 17], the small-scale structure inferred from Lyman- α observations [14], and the velocity dispersion in dwarf spheroids [16].

II. MAJORANA MASSES FROM AN EXTENDED HIGGS SECTOR

Although the Standard Model was originally formulated with massless neutrinos ν_i transforming as components of the electroweak $SU(2)$ doublets L_α ($\alpha = 1, 2, 3$), the neutrino masses can be accommodated by a relatively

minor modification. One adds several electroweak singlets N_a ($a = 1, \dots, n$) to the Standard Model and builds a seesaw lagrangian [1]:

$$\mathcal{L} = \mathcal{L}_{\text{SM}} + i\bar{N}_a \not{\partial} N_a - y_{\alpha a} H \bar{L}_\alpha N_a - \frac{M_a}{2} \bar{N}_a^c N_a + h.c. \quad (1)$$

The neutrino mass eigenstates $\nu_i^{(\text{m})}$ ($i = 1, \dots, n+3$) are linear combinations of the weak eigenstates $\{\nu_\alpha, N_a\}$. They are obtained by diagonalizing the mass matrix:

$$\begin{pmatrix} 0 & y_{\alpha a} \langle H \rangle \\ y_{a\alpha} \langle H \rangle & \text{diag}\{M_1, \dots, M_n\} \end{pmatrix} \quad (2)$$

As long as all $y_{\alpha a} \langle H \rangle \ll M_a$, the eigenvalues of this matrix split into two groups: the lighter states with masses of the order of $y_{\alpha a}^2 \langle H \rangle^2 / M_a$, and the heavier eigenstates with masses of the order of M_a . As usual, we will call the former *active neutrinos* and the latter *sterile neutrinos*. The mixing angles in this case are of the order of $\theta_{\alpha a}^2 \sim y_{\alpha a}^2 \langle H \rangle^2 / M_a^2$.

The number n of the right-handed singlets is unknown, although it is clear that $n \geq 2$ is a necessary condition to explain the results from the atmospheric and solar neutrino experiments [21]. Theoretical considerations do not constrain the number n of sterile neutrinos. In particular, there is no constraint based on the anomaly cancellation because the sterile fermions do not couple to the gauge fields. The experimental limits exist only for the larger mixing angles [25]. The scale of the right-handed Majorana masses, M_a , can vary over many orders of magnitude. It can be much greater than the electroweak scale [1], or it may be as low as a few eV [26]. It is also possible that some of the right-handed Majorana masses are much larger than others. The seesaw mechanism can explain the smallness of the neutrino masses even if the Yukawa couplings are of order one, as long as the Majorana masses M_a are large enough. However, the origin of the Yukawa couplings remains unknown. If the Yukawa couplings arise as some topological intersection numbers in string theory, they are generally expected to be of order one [27], although very small couplings can be also possible [28]. However, if the Yukawa couplings arise from the overlap of the wavefunctions of fermions located on different branes in extra dimensions, they can be exponentially suppressed and are expected to be very small [29]. If one or more singlets have Majorana masses below the electroweak scale, they can appear as sterile neutrinos and can have important ramifications; for example, dark matter can be made up of sterile neutrinos with mass of several keV [2], and the same particle can be responsible for the observed pulsar kicks [9].

Several recent papers have studied in detail one particular case, named νMSM [5], which corresponds to $n = 3$, $M_1 \sim \text{keV}$, and $M_2 \approx M_3 \sim 1 - 10 \text{ GeV}$. In this model, the keV sterile neutrino serves as the dark matter particle (and can explain the pulsar kicks), while the degenerate heavier states, $M_2 \approx M_3$, make the model is amenable to leptogenesis by neutrino oscillations [30].

The possible role of keV sterile neutrinos in astrophysics and cosmology, from dark matter to pulsar kicks, to early star formation, makes the possibility of their existence very intriguing. However, if the neutrino Majorana masses M_a are below the electroweak scale, one should try to explain the origin of this scale. The other fermions in the same mass range acquire their masses from the Higgs mechanism. Can the mass terms in eq. (1) also arise from the Higgs mechanism? The answer is yes; this requires an extension of the Higgs sector by an $\text{SU}(2)$ singlet field coupled to the right-handed fermions as in Refs. [6, 7, 20]:

$$\begin{aligned} \mathcal{L} = & \mathcal{L}_{\text{SM}} + i\bar{N}_a \not{\partial} N_a - y_{\alpha a} H \bar{L}_\alpha N_a - \frac{f_a}{2} S \bar{N}_a^c N_a \\ & - V(H, S) + h.c. \end{aligned} \quad (3)$$

We will assume that S is a real scalar field to avoid the light Nambu-Goldstone bosons associated with the breaking of the lepton number $\text{U}(1)$; the presence of such light bosons would render the sterile neutrinos unstable, hence they could not be dark matter (although they could still explain the pulsar kicks [9]). If the singlet has very small mass and a large VEV, it can be the inflaton [6]. We will not discuss this interesting possibility here, but we will concentrate instead on a singlet Higgs whose mass and VEV are both of the order of 100 GeV, which, incidentally, is the requirement for the keV dark matter, as long as the mass and VEV of S are of the same order of magnitude [7].

As soon as the SNN coupling is introduced in the lagrangian, there appears a new way in which the relic population of sterile neutrinos can be produced, namely from the decays $S \rightarrow NN$. This decay mechanism can operate in addition to the neutrino oscillations mechanism of Dodelson and Widrow [2], and one has to compare the relative amounts produced by each of them. Another important issue is how cold the dark matter is if it is produced predominantly from the Higgs decays. Since the production occurs mainly at temperatures of the order of the Higgs mass, $T \sim 100 \text{ GeV}$, the reduction in the number of degrees of freedom and the entropy production that takes place as the universe cools down from $T \sim 100 \text{ GeV}$ causes the dark matter population to be diluted and red shifted by a factor $\xi \geq 33$ in the density and factor $\xi^{1/3} \geq 3.2$ in the average momentum. These values reflect only the Standard Model degrees of freedom, and any additional new physics will make ξ even larger. The corresponding free-streaming length is shorter, and the Lyman-alpha bounds become proportionately weaker [7].

In this paper we discuss the details of sterile dark matter production in a model represented by the lagrangian (3), with the scalar potential

$$\begin{aligned} V(H, S) = & -\mu_H^2 |H|^2 - \frac{1}{2} \mu_S^2 S^2 + \frac{1}{6} \alpha S^3 + \omega |H|^2 S \\ & + \lambda_H |H|^4 + \frac{1}{4} \lambda_S S^4 + 2\lambda_{HS} |H|^2 S^2 \end{aligned} \quad (4)$$

III. STERILE DARK MATTER: COLD OR WARM?

If dark matter has a non-zero free-streaming length, the structure on small scales may be suppressed. Studies of small-scale structure based on the observations of dwarf Spheroids [16] or Lyman- α forest data [14] can constrain or measure the free-streaming length of the dark-matter particles, but the relation between this length and the particle mass depends on the production mechanism. One can approximately relate the free-streaming length to the mass m_s and the average momentum of the sterile neutrino:

$$\Lambda_{FS} \approx 1.2 \text{ Mpc} \left(\frac{\text{keV}}{m_s} \right) \left(\frac{\langle p_s \rangle}{3.15 T} \right)_{T \approx 1 \text{ keV}} \quad (5)$$

This is a relatively good measure in many cases, although in general one has to calculate the full power spectrum. The observations of Lyman- α forest constrain the free-streaming length to be less than 0.11 Mpc [14]. This bound does not translate directly into a constraint on the mass because the average momentum depends on the production mechanism. For three scenarios usually discussed in the literature,

$$\left(\frac{\langle p_s \rangle}{3.15 T} \right)_{T \approx \text{keV}} = \begin{cases} 0.9, & \text{for DW} \\ 0.6, & \text{for } L \neq 0, \text{resonance} \\ 0.2, & \text{for } T_{\text{prod}} \gtrsim 100 \text{ GeV} \end{cases} \quad (6)$$

Here DW stands for Dodelson-Widrow production mechanism via non-resonant neutrino oscillations [2], “ $L \neq 0$ ” refers to the Shi-Fuller production via the resonant neutrino oscillations in the case when the lepton asymmetry is relatively large [4], and “ $T_{\text{prod}} \gtrsim 100 \text{ GeV}$ ” refers to the production of sterile neutrinos at a temperature well above the QCD scale, in which case the cooling and reduction of the degrees of freedom causes the red shift in the population of dark matter [7].

For the same mass, the sterile dark matter can be colder or warmer, depending on the production mechanism. This is clear from equations (5) and (6), which, for a given cosmological scenario, relate the free-streaming length with the mass. Therefore, we will pay close attention to the factors that can affect the momentum distribution in each scenario.

There are several ways in which the population of dark matter particles could have formed in our model:

- The bulk of sterile neutrinos could be produced from neutrino oscillations. If the lepton asymmetry is negligible, this scenario [2] appears to be in conflict with a combination of the X-ray bounds [13] and the Lyman- α bounds [15], although it is possible to evade this constraint if the lepton asymmetry of the universe is greater than 10^{-3} [4]. It is possible that the decays of additional, heavier sterile neutrinos, can introduce some additional entropy and contribute to cooling of dark matter [22]. It is

also possible that the sterile neutrinos make up only a fraction of dark matter [7, 15], in which case they can still be responsible for the observed velocities of pulsars.

- The bulk of sterile neutrinos could be produced from decays of S bosons at temperatures of the order of the S boson mass, $T \sim 100 \text{ GeV}$. This scenario was discussed in Ref. [7]. In this case, the Lyman- α bounds on the sterile neutrino mass are considerably weaker than in the former case.
- The decays described above could happen before a first-order phase transition, and the entropy release in the transition could redshift the population of the dark-matter particles. We have explored this possibility in detail, as discussed below, but we have not found a range of parameters in which the phase transition could cool down the sterile dark matter significantly.
- S bosons could be so weakly coupled to the rest of the Higgs sector that they would go out of equilibrium and decay out of equilibrium at some temperature $T < 100 \text{ GeV}$. As discussed below, this scenario can produce a sufficient amount of dark matter.

We will now discuss these possibilities in detail.

IV. PRODUCTION FROM THE HIGGS DECAYS IN EQUILIBRIUM

The interactions of the singlet Higgs bosons with SM particles have been studied by McDonald in Ref. [23], where the S bosons were made stable by imposing a global U(1) symmetry, which removed the odd power couplings, and by setting $\mu_s^2 < 0$, which forced $\langle S \rangle = 0$. In this case, the coupling λ_{HS} controls the $SS \rightarrow XX$ annihilations, into SM fermions and the W, Z bosons. We do not require S to be stable. After S develops a VEV, other couplings also contribute to the annihilations into SM particles. For each of these processes the cross section for annihilation is:

$$\sigma_{\text{ann}} \sim 10^{-2} \frac{\lambda_{HS}^2}{m_S^2} \quad (7)$$

At some temperature, these processes fail to keep the S particles in equilibrium, and they freeze out at $T_f = m_S/r_f$. For very small $\lambda_{HS} \lesssim 10^{-6}$, S bosons never come into equilibrium. A more detailed numerical calculation yields the dependence of the freeze-out time parameter r_f on λ_{HS} shown in fig. 1.

The cubic couplings contribute to the annihilation processes through exchange of virtual S bosons. In fact, this will be the dominant process that keeps S particles in equilibrium, as long as $\frac{\alpha\omega}{m_S^2} \gtrsim \lambda_{HS}$, where m_S is the S boson mass. Comparing with Fig. 1, one can see that

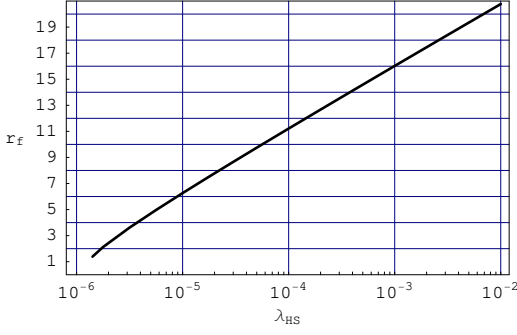


FIG. 1: The variation of the S boson freeze-out parameter $r_f = m_S/T_f$ with the coupling to SM particles λ_{HS} . For numerical estimations we used $m_S = 200$ GeV.

this process can keep S bosons in equilibrium down to rather low temperatures, even if α, ω are well below the S mass.

Let us now assume that the α, ω and/or λ_{HS} are large enough (exact limit for λ_{HS} to be defined below) to keep S in equilibrium down to temperatures well below its mass. One can make a rough estimate of the sterile neutrino production by multiplying the S number density by the $S \rightarrow NN$ decay rate $\Gamma = f^2 m_S / (16\pi)$ and by the time available for the decay, $\tau \sim M_0 / 2T^2$, at the latest temperature at which the thermal population of S is still significant, namely $T \sim m_S$. At lower temperatures, the S number density is too small, much smaller than T^3 . One obtains an approximate result

$$\left(\frac{N_s}{T^3} \right) \Big|_{T \sim m_S} \sim \Gamma \frac{M_0}{T^2} \Big|_{T \sim m_S} \sim \frac{f^2}{16\pi} \frac{M_0}{m_S}, \quad (8)$$

where $M_0 = \left(\frac{45 M_{PL}^2}{4\pi^3 g_*} \right)^{1/2} \sim 10^{18}$ GeV is the reduced Planck Mass.

This simple estimate is in agreement with the solution of the kinetic equation discussed below. Of course, this description breaks down if the S particles decouple and decay at a much later time. We will come back to this possibility. For now, let us assume that S particles maintain their equilibrium populations down to temperatures at least a factor of a few below their masses. The dark matter abundance for sterile neutrinos from the decay of bosonic particles in equilibrium was first computed for a model in which the S field served as the inflaton with a potential adjusted to have $\langle S \rangle \gg m_S$ [6]. The results of this computation carry over to our case. Here we do not require S to be the inflaton, and we take $\langle S \rangle \sim m_S$, as in Ref. [7]. As was shown in Ref. [7], the choice $\langle S \rangle \sim m_S$, along with the requirement that sterile neutrinos make up all the dark matter, force the S boson mass and VEV to be right at the electroweak scale, $\langle S \rangle \sim m_S \sim 10^2$ GeV, suggesting that S may, indeed, be a part of the Higgs sector of the extended Standard Model, and justifying some of our assumptions regarding the Higgs potential.

Dark matter production from particle decays has been considered in a number of papers [6, 24]. Let us first

consider the decaying particle in equilibrium. As in the case of the inflaton decay [6], the sterile neutrino distribution function $n(p, t)$ is found from the following kinetic equation:

$$\frac{\partial n}{\partial t} - Hp \frac{\partial n}{\partial p} = \frac{2m_S \Gamma}{p^2} \int_{p+\frac{m_S}{4p}}^{\infty} n_S dE, \quad (9)$$

where $\Gamma = m_S f^2 / 16\pi$ is the partial width of the S boson decay. It is assumed that the sterile neutrinos are never in equilibrium, and the inverse decays $NN \rightarrow S$ can be neglected, which is true for small Yukawa couplings $f < 10^{-7}$. Transforming to the variables: $r = \frac{m_S}{T}$, $x = \frac{p}{T}$, one can rewrite eq. (9):

$$\frac{\partial n}{\partial r} = \frac{f^2 M_0}{8\pi m_S} \frac{r^2}{x^2} \int_{x+\frac{r^2}{4x}}^{\infty} n_S \Big|_{\frac{E}{T}=\zeta} d\zeta. \quad (10)$$

Since S and H mix, one has to consider the mixed mass eigenstates in plasma. Both of them can decay into sterile neutrinos. The SM Higgs is in thermal equilibrium due to the coupling with the SM particles. For the temperature range in which S is also in equilibrium, the distribution functions of the two mass eigenstates will be:

$$n_j = \frac{1}{e^{E_j/T} - 1} \quad (11)$$

Then eq. (10) yields:

$$\begin{aligned} n^\Theta(x, r) = & \sum_{j=1}^2 \frac{f_j^2 M_0}{8\pi m_j} \left[\frac{r_j^3}{3x^2} \ln \left(1 - e^{-x - \frac{r_j^2}{4x}} \right)^{-1} \right. \\ & \left. + \frac{8x^2}{3} \int_1^{1+\frac{r_j^2}{4x^2}} \frac{(z-1)^{3/2} dz}{e^{xz} - 1} \right] \end{aligned} \quad (12)$$

where the subscript $j = 1, 2$ runs over the two Higgs mass eigenstates and the superscript Θ denotes production from decays of S bosons in equilibrium. (We will use \emptyset for the case of S bosons decaying out of equilibrium.) In (12) the first term is important when $r \lesssim 1$, while the second is the dominant one for $r \gtrsim 1$. The above solution was obtained assuming f_j, m_j and the number of degrees of freedom g_* remain constant. This is not valid after the electroweak phase transition takes place, since the Higgs mass eigenvalues and their mixing are different in the two vacua. If f_j, m_j or g_* change at some points in the evolution of the universe, the solution has to be adjusted to include the contributions from all the periods corresponding to different f_j, m_j, g_* . Each of these contributions will still be given by (12), for the appropriate values of the parameters and taken over the respective time intervals.

This complication turns out to be irrelevant, since the production rate of sterile neutrinos through each mode m_j exhibits a well-defined peak at $r_j \simeq 2.3$, which defines the production temperature $T_{\text{prod}} = m_j / 2.3$. Most of the sterile neutrinos are produced around that temperature,

and by the time when $r_j \approx 10$ the production of sterile neutrinos though m_j decays has practically been completed. More specifically, in the simplified case $m_1 \ll m_2$, $f_1 \gg f_2$, m_1 decays will dominate over m_2 decays and the total abundance of sterile neutrinos $Y_s = N_s/s$ at any later temperature will be:

$$Y_s^\Theta(r) = \frac{45}{32\pi^5} \frac{f^2}{g_*(T_{\text{prod}})} \frac{M_0}{m} y(r) \quad (13)$$

where

$$y(r) = \frac{1}{3} \int_0^\infty dx \left[r^3 \ln \left(1 - e^{-x - \frac{r^2}{4x}} \right)^{-1} + 8x^4 \int_1^{1 + \frac{r^2}{4x^2}} \frac{(z-1)^{3/2} dz}{e^{xz} - 1} \right] \quad (14)$$

and we have dropped the mass eigenstate index for simplicity. The $g_*(T_{\text{prod}})^{-1}$ factor in (13) designates the fact that the sterile neutrino population will be diluted by

$$\xi = g_*(T_{\text{prod}})/g_*(0.1 \text{ MeV}) \quad (15)$$

as the universe cools down, due to the entropy release as the effective degrees of freedom decrease. At $r \rightarrow \infty$, the sterile neutrino abundance produced from in-equilibrium decays takes the limiting value:

$$Y_s^\Theta(\infty) = \frac{27\zeta(5)}{32\pi^4} \frac{f^2}{g_*(T_{\text{prod}})} \frac{M_0}{m}. \quad (16)$$

We require that the decays of S bosons occur in equilibrium, that is $T_f \lesssim \frac{m}{10}$. Then we get from Fig. 1, $\lambda_{HS} \gtrsim 5 \cdot 10^{-5}$, for $\alpha = \omega = 0$. However, if $\alpha, \omega \gtrsim 1 \text{ GeV}$ S bosons stay in equilibrium down to the desired temperature, regardless of λ_{HS} .

The momentum distribution in eq. (12) is non-thermal. Taking into account only the dominant decay mode, one obtains (same as in Ref. [6]) the momentum distribution of dark-matter particles at $r \rightarrow \infty$:

$$n^\Theta(x) = \frac{f^2 M_0}{3\pi m} x^2 \int_1^\infty \frac{(z-1)^{3/2} dz}{e^{xz} - 1}, \quad (17)$$

for which the average momentum at temperature $T \sim 10^2 \text{ GeV}$, immediately after their production, is (cf. Ref. [6])

$$\left(\frac{\langle p \rangle}{T} \right)_{T \sim 100 \text{ GeV}} = \frac{\pi^6}{378 \zeta(5)} \simeq 2.45. \quad (18)$$

This is lower than the same quantity for a thermal distribution, $\langle p \rangle/T = 3.15$.

Even more importantly, these momenta are further redshifted as the universe cools down from the temperature at which most dark matter is produced, $T_{\text{prod}} \sim m \sim 100 \text{ GeV}$ to the much lower temperatures at which the structure begins to form. As the universe cools down, the number of effective degrees of freedom decreases from

$g_*(T_{\text{prod}}) = 110.5$ to $g_*(0.1 \text{ MeV}) = 3.36$. This assumes no new physics below the Higgs mass; any new physics would cause an additional cooling of the dark matter. The ratio of dark matter to entropy is reduced by the factor $\xi \approx 33$. This causes the redshifting of $\langle p_s \rangle$ by the factor $\xi^{1/3}$:

$$\left(\frac{\langle p \rangle}{T} \right)_{(T \ll 1 \text{ MeV})} = 0.76 \left[\frac{110.5}{g_*(\tilde{m}_s)} \right]^{1/3}. \quad (19)$$

This is very different from the DW scenario [2], in which the average neutrino momentum at low temperature T is

$$\langle p_s \rangle_{\text{DW}} = 2.83 T. \quad (20)$$

Comparing eqns. (20) and (19), one concludes that the sterile neutrino mass corresponding to the same free-streaming length can vary by more than a factor of 3 depending on the production scenario [7].

The dark matter abundance in this model depends on the details of the Higgs mass matrix and the two-component decays, aside from which it has the form:

$$\Omega_{\nu_s} \sim 0.2 \left(\frac{f}{10^{-8}} \right)^3 \left(\frac{\langle S \rangle}{m_{1,2}} \right) \left(\frac{33}{\xi} \right). \quad (21)$$

Since we expect the masses of the two mass eigenstates to be of the same order, and considering the cubic power of the unknown coupling f , the details of the solution are not very important. However, what may be important is the additional effect of the first-order phase transition on the average momentum of the dark matter particles. If the dark matter population is redshifted significantly by the entropy release in the phase transition, then the Lyman- α bound could be further relaxed.

V. ELECTROWEAK PHASE TRANSITION

As discussed above, the population of sterile neutrinos is subject to dilution and redshift due to the entropy production that occurs (i) in any possible phase transitions at lower temperatures, and (ii) when the number of degrees of freedom in plasma decreases due to the decoupling of Standard model particles below 100 GeV. The redshift due to (ii) alone can reduce the momenta of dark matter particles by a factor more than 3.2 [7]. Of course, the dilution due to (i) matters only if a first-order phase transition takes place after the sterile neutrinos are produced, and, moreover, if S bosons are too heavy to have a high number density in the new vacuum after the phase transition. To study this possibility, one has to take into account the temperature effects on the effective potential and the history of the phase transitions predicted by the model. Electroweak phase transition in a model with a singlet Higgs has been analyzed in Refs. [34, 35, 36]. The plausibility of the first-order phase transition makes the electroweak baryogenesis a viable possibility, and it has implications for the LHC and the ILC [36]. Here we concentrate on the effects the first-order transition could have on the population of dark-matter sterile neutrinos.

A. Finite-temperature effects and the first-order phase transition

The tree level effective potential in terms of the VEV of the two Higgs bosons, $\langle H \rangle = \frac{1}{\sqrt{2}}\eta$ and $\langle S \rangle = \sigma$ is

$$V_{\text{tree}}^0(\eta, \sigma) = -\frac{1}{2}\mu_H^2\eta^2 + \frac{\lambda_H}{4}\eta^4 - \frac{1}{2}\mu_S^2\sigma^2 + \frac{\lambda_S}{4}\sigma^4 + \lambda_{HS}\eta^2\sigma^2 + \frac{\alpha}{6}\sigma^3 + \frac{\omega}{2}\eta^2\sigma \quad (22)$$

To study the phase transition, we included the one-loop temperature-dependent corrections and analyzed the potential numerically, as discussed below.

The tree level Higgs mass eigenvalues are:

$$\begin{aligned} (m_{1,2}^0)^2 &= \frac{1}{2}[(3\lambda_H + 2\lambda_{HS})\eta^2 + (3\lambda_S + 2\lambda_{HS})\sigma^2 \\ &+ (\omega + \alpha)\sigma - \mu_H^2 - \mu_S^2 \\ &\pm \{(3\lambda_H - 2\lambda_{HS})\eta^2 - (3\lambda_S - 2\lambda_{HS})\sigma^2 \\ &+ (\omega - \alpha)\sigma - \mu_H^2 + \mu_S^2\}^2 \\ &+ 4\eta^2(4\lambda_{HS}\sigma + \omega)^2]^{1/2} \end{aligned} \quad (23)$$

The 1-loop, zero temperature correction to the effective potential [31] in the \overline{MS} renormalization scheme is:

$$V^1(\eta, \sigma) = \sum_i \frac{n_i}{64\pi^2} m_i^4(\eta, \sigma) \left(\log \frac{m_i(\eta, \sigma)^2}{m_i(\eta_0, \sigma_0)^2} - \frac{3}{2} \right) \quad (24)$$

where n_i are the degrees of freedom of the contributing particles and $m_i(\eta, \sigma)$ are their field-dependent masses. The main contributions are from the neutral component of the SM Higgs, the singlet Higgs, the Goldstone bosons χ , the W and Z gauge bosons and the top quark t :

$$n_t = -12, n_W = 6, n_Z = 3, n_\chi = 3, n_H = n_S = 1 \quad (25)$$

The Higgs-singlet S does not couple to the fermions or the gauge bosons, thus their field dependent masses are the same as in the minimal SM :

$$\begin{aligned} m_t^2 &= \frac{y_t^2}{2}\eta^2, m_W^2 = \frac{g^2}{4}\eta^2, m_Z^2 = \frac{g^2 + g'^2}{4}\eta^2, \\ m_\chi^2 &= \lambda_H\eta^2 - \mu_H^2 + 2\lambda_{HS}\sigma^2 + \omega\sigma \end{aligned} \quad (26)$$

The Higgs mass eigenvalues are given by (23). $m_i(\eta_0, \sigma_0)$ stand for particle masses at the vacuum state (η_0, σ_0) at zero temperature.

The temperature-dependent contribution to the effective potential at one loop is [32, 33]:

$$V^T(\eta, \sigma, T) = \sum_i \frac{n_i T^4}{2\pi^2} I_{b,f} \left(\frac{m_i^2(\eta, \sigma)}{T^2} \right) + V_{\text{ring}}^T \quad (27)$$

where

$$I_{b,f}(y) = \int_0^\infty dx x^2 \log [1 \mp e^{-\sqrt{x^2+y}}] \quad (28)$$

The upper sign corresponds to bosons, while the lower one to fermions. Since we consider a wide range of temperatures, we do not make use of the well known high- T expansion of the functions (28). V_{ring}^T is the ring contribution of the gauge, Higgs and goldstone bosons:

$$\begin{aligned} V_{\text{ring}}^T &= -\frac{T}{12\pi} \left\{ \text{Tr} [(m_{gb}^2 + \Pi_{gb})^{3/2} - (m_{gb}^2)^{3/2}] \right. \\ &+ \text{Tr} [(m_{\text{higgs}}^2 + \Pi_{\text{higgs}})^{3/2} - (m_{\text{higgs}}^2)^{3/2}] \\ &+ n_\chi [(m_\chi^2 + \Pi_\chi)^{3/2} - (m_\chi^2)^{3/2}] \left. \right\} \end{aligned} \quad (29)$$

where m_{higgs} is the tree level Higgs mass mixing matrix, corresponding to the potential (22), whose eigenvalues are given in (23). m_{gb}^2 is the mass mixing matrix for the electroweak gauge bosons:

$$m_{\text{gb}}^2 = \begin{pmatrix} \frac{g^2\eta^2}{4} & 0 & 0 & 0 \\ 0 & \frac{g'^2\eta^2}{4} & 0 & 0 \\ 0 & 0 & \frac{g^2\eta^2}{4} & -\frac{gg'\eta^2}{4} \\ 0 & 0 & -\frac{gg'\eta^2}{4} & \frac{g'^2\eta^2}{4} \end{pmatrix} \quad (30)$$

Π_i are the thermal contributions to the masses, given for our model by [33, 34, 36]:

$$\begin{aligned} \Pi_{\text{gb}} &= \text{diag} \left[\frac{11}{6}g^2T^2, \frac{11}{6}g'^2T^2, \frac{11}{6}g^2T^2, \frac{11}{6}g'^2T^2 \right] \\ \Pi_{\text{higgs}} &= \text{diag} \left[\left(\frac{3}{16}g^2 + \frac{1}{16}g'^2 + \frac{\lambda_H}{2} + \frac{y_t}{4} + \frac{\lambda_{HS}}{3} \right) T^2, \right. \\ &\quad \left. \left(\frac{1}{4}\lambda_S + \frac{4}{3}\lambda_{HS} \right) T^2 \right] \\ \Pi_\chi &= \left(\frac{3}{16}g^2 + \frac{1}{16}g'^2 + \frac{\lambda_H}{2} + \frac{y_t}{4} + \frac{\lambda_{HS}}{3} \right) T^2 \end{aligned} \quad (31)$$

The effective potential at finite temperature is the sum of (22), (24) and (27):

$$V_{\text{eff}}(\eta, \sigma, T) = V^0(\eta, \sigma) + V^1(\eta, \sigma) + V^T(\eta, \sigma, T) \quad (32)$$

In the calculations that follow we ignore V^1 for simplicity, since it is only a small correction to the zero- T effective potential, and we treat the imaginary part of the potential as usual [40].

The history of the universe for a typical set of parameters discussed in table I, is shown in fig. 2. Due to the symmetry $\eta \rightarrow -\eta$, only the $\eta > 0$ half plane need to be considered.

Since the singlet does not couple to the gauge bosons and the t quark, it receives the smallest correction at a high temperature. Therefore, there is usually a range of temperatures in which the Higgs doublet has no VEV, while the singlet has a VEV. At a higher temperature, the singlet VEV also tends to 0, although it never completely disappears due to the $\sigma \rightarrow -\sigma$ asymmetry, induced by the α and ω terms.

Therefore, in the early universe, at $T \gg 100$ GeV, the effective potential has a unique minimum at $\{0, \sigma_f\}$. At

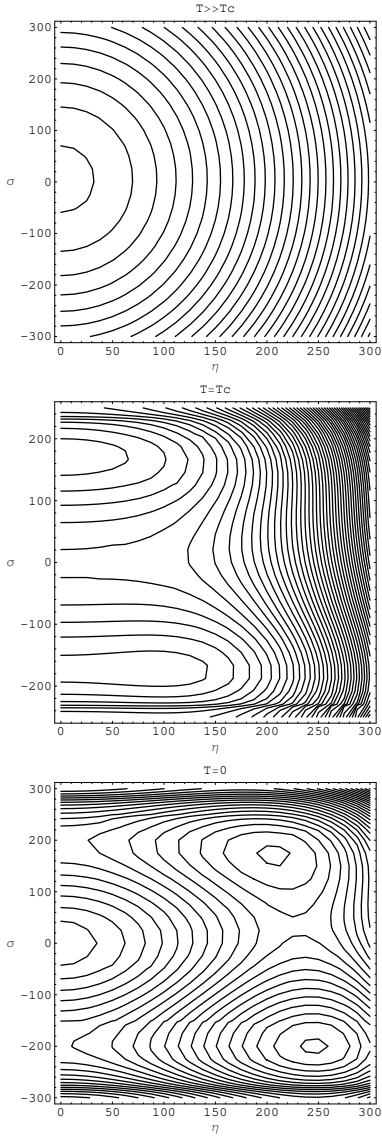


FIG. 2: Contour plots of $V_{\text{eff}}(\eta, \sigma, T)$ at $T \gg T_c$, $T = T_c$, and $T = 0$, corresponding to the parameter set A of table I. At $T \gg T_c$ the universe is in the unbroken phase $\eta = 0$, with $\sigma > 0$. At lower temperatures, the minimum of V_{eff} shifts to non-zero η , while a second minimum appears in the $\sigma < 0$ region. The two minima become degenerate at $T = T_c$, and at $T = 0$ the true vacuum is located at $\eta = 246$ GeV, $\sigma < 0$.

a lower temperature, for some range of the parameter space, the doublet also develops a VEV and the universe shifts to $\{\eta_f(T), \sigma_f(T)\}$ through a second order phase transition. In the meanwhile, a local minimum has been developed at $\{\eta_t(T), \sigma_t(T)\}$. At $T = T_c$ the two minima become degenerate and at $T < T_c$, $\{\eta_t, \sigma_t\}$ turns out to be the true vacuum (*cf.* Fig. 2). At some temperature $T_o \lesssim T_c$ the false vacuum decays into the true vacuum via bubble nucleation, described in section VB. Fig. 3 shows this evolution along the straight-line path connecting the two minima, as universe cools down. In Fig. (4),

we show the evolution of the order parameter, the SM Higgs VEV η .

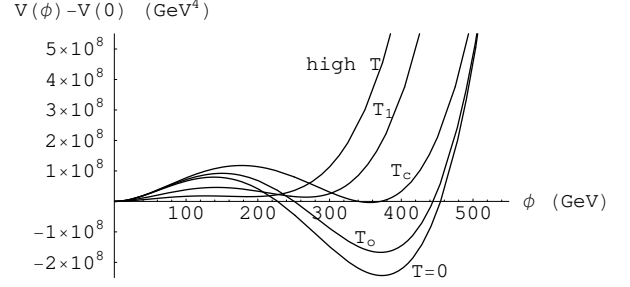


FIG. 3: The potential configuration along the straight-line path connecting the two minima, at various temperatures. At very high T the potential possesses only one minimum. At a lower temperature T_1 a local minimum starts forming. At $T_c < T_1$ the two minima become degenerate. At $T_o < T_c$ tunneling to the true vacuum occurs. At $T = 0$ the universe has settled in the true vacuum. The curves correspond to parameter set A of table I.

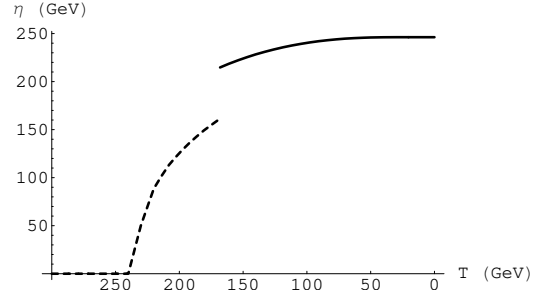


FIG. 4: The evolution of the SM Higgs VEV η with temperature. At very high T , symmetry is restored: $\eta = 0$. At a lower temperature a second order phase transition to $\eta \neq 0$ takes place, while still remaining in the false vacuum (dashed line). At $T = T_o$, a first order phase transition brings the universe to the true vacuum (solid line). At $T = 0$, $\eta = 246$ GeV. The data corresponds to parameter set A of table I.

B. Phase Transition through Bubble Nucleation

The tunneling from the false to the true vacuum was calculated numerically using an approximation in which the bounce [37] was assumed to lie along a straight line in the 2-d field space (η, σ) . Let ϕ be the field configuration along this path. At finite temperature, one looks for solutions of the Euclidean equations periodic in the “time” direction with period T^{-1} [38]. In the high-temperature limit, the solution should be translationally invariant along the “time” axis, thus the dependence of ϕ

on temperature disappears. The $O(3)$ -symmetric (in the spatial coordinates) solution will now obey the equations:

$$\frac{d^2\phi}{dr^2} + \frac{2}{r}\frac{d\phi}{dr} = \frac{dV}{d\phi}, \quad \left.\frac{d\phi}{dr}\right|_{r=0} = 0, \quad \phi(\infty) = 0, \quad (33)$$

where $\phi = 0$ is the false vacuum. The decay rate per unit volume is

$$\Gamma \approx T^4 \left(\frac{S_3(T)}{2\pi T} \right)^{3/2} e^{-S_3/T}, \quad (34)$$

where we neglect the prefactor due to the change in the symmetry group [39]. Here $S_3[\phi]$ is the 3-dimensional action:

$$S_3[\phi] = \int d^3x \left[\frac{1}{2} (\nabla\phi)^2 + V(\phi, T) \right]. \quad (35)$$

For the solution of eq. (33) we adopt numerical methods, rather than using the well-known approximation schemes at the thin and thick wall limits [38]. The O_4 symmetric case at $T = 0$ has been solved numerically in [41]. We do the same for the O_3 symmetric equation (33) and present here the results, used for the numerical estimates of table I.

A potential of the form:

$$V(\phi) = \frac{1}{2}M(T)^2\phi^2 - \frac{1}{3}\delta(T)\phi^3 + \frac{1}{4}\zeta(T)\phi^4 \quad (36)$$

with $M^2 > 0$ to ensure at least metastability at $\phi = 0$, encompasses all of the renormalizable potentials. For such a potential the transition between different regions depends on a single dimensionless parameter:

$$\kappa = \frac{9}{8} \frac{\zeta M^2}{\delta^2} \quad (37)$$

For tunneling to occur we must have $\kappa \leq \frac{1}{4}$, while $\kappa \geq 0$ is required for the potential to be bounded from below.

At finite temperature, the O_3 symmetric action (35) is found to be:

$$S_3 = \frac{9M^3}{2^{3/2}\delta^2} \times \left[\hat{S}_{3,\text{thick}} + 125.8\kappa - 239.5\kappa^2 + \frac{33\kappa}{1-4\kappa} + \hat{S}_{3,\text{thin}} \right] \quad (38)$$

with $\hat{S}_{3,\text{thick}} \simeq 13.72(1-4\kappa)^2$ and $\hat{S}_{3,\text{thin}} = \frac{2^4\sqrt{2}\pi}{3^6} \frac{4\kappa}{(1-4\kappa)^2}$ being the limits for the thick and thin wall approximation, respectively [38].

The time needed for the universe to tunnel from the false to the true vacuum is estimated by setting $\Gamma \cdot t_H^4 \approx 1$ where $t_H = \frac{M_0}{2T^2}$ is the Hubble time in the radiation-dominated universe. Taking into account that during the electroweak phase transition $T \approx 100$ GeV, this yields: $\frac{S_3}{T} \approx 160$, which defines the tunneling temperature T_o in the estimations of table I. If $\frac{S_3}{T} \ll 160$, the tunneling

occurs very quickly, when the universe is still hot. If $\frac{S_3}{T} \gg 160$, the tunneling rate is too low and the universe remains at the false vacuum.

When this condition is met, the universe tunnels from the false vacuum ϕ_f to the true vacuum ϕ_t . The energy gained from the transition to a deeper minimum reheats the universe from the tunneling temperature T_o to a higher temperature T_r . Since the expansion of the universe is much slower than the tunneling, the reheating temperature T_r is found by taking the energy density to be constant $\rho(\phi_f(T_o), T_o) = \rho(\phi_t(T_r), T_r)$, where $\rho(\phi, T) = f(\phi, T) + T s(\phi, T)$, with $f(\phi, T) = V_{\text{eff}}(\phi, T)$ the free energy density and $s = -\partial f / \partial T$ the entropy density. In fig.5 the free energy density in the true and false vacuum are presented vs temperature.

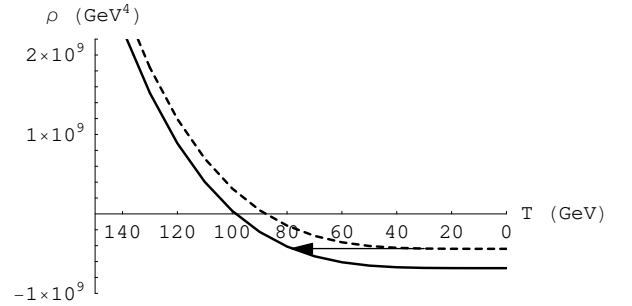


FIG. 5: The free energy density vs temperature, at the true vacuum (lower curve) and at the false vacuum (upper curve). Significant reheating could occur if the universe cooled down to a low temperature before the tunneling took place. At the temperature at which the tunneling actually occurs, $T \approx 100$ GeV, the reheating is not significant.

Representative numerical estimations done using the above are presented in table I. The independent parameters of the model were chosen to be $\lambda_H, \lambda_S, \lambda_{HS}, \alpha, \omega$ and the VEVs of the two Higgs bosons at zero temperature η_0, σ_0 , of which η_0 is kept fixed at 246 GeV.

T_c, T_o, T_r stand for the critical, tunneling and reheating temperature respectively. v_c is the distance between the two vacua at the critical temperature and $\frac{v_c}{T_c} > 1$ is the criterion for a strong 1st order phase transition. The parameter space of the potential (4) can provide for a variety of phase transition scenarios (1st order only, 2nd order only, 2nd order followed by 1st order). The parameter sets presented here fulfill the requirement for a strong 1st order P.T. In A, a second order phase transition to non-zero VEV of the SM Higgs precedes the first order one to the true vacuum (fig. 4). In B, no second-order phase transition occurs.

$m_{1,2}^t(T), m_{1,2}^f(T)$ stand for the Higgs mass eigenvalues at the true and false vacuum respectively, at temperature T . For the parameter sets of table I, both of the Higgs modes decay after the transition to the true vacuum, since $T_r > \frac{m_{1,2}^t(T_r)}{2.3}$, which is the temperature

parameter sets	A	B
λ_H	0.5	0.6
λ_S	0.6	0.4
λ_{HS}	0.025	-0.02
α	2	-25
ω	25	90
σ_0	-200	-220
T_c	266	220
T_o	168	179
T_r	170	182
v_c/T_c	1.4	1.5
$m_{1,2}^t(0)$	227, 247	188, 302
$m_{1,2}^f(T_o)$	191, 139	118, 101
$m_{1,2}^t(T_r)$	215, 201	251, 143
$\langle p \rangle/T$	0.84	0.85
f	$4.2 \cdot 10^{-8}$	$4 \cdot 10^{-8}$
m_s (keV)	8.42	8.85

TABLE I: Representative parameter sets (see text for discussion). The unit for all dimensionfull parameters is GeV, except for m_s , which is given in keV.

at which the decay rate appears to be maximal. Conversely, decay in the false vacuum would require tunneling temperature small enough, $T_o < \frac{m^f(T_o)}{2.3}$, in order for the Higgs bosons to have time to decay before the phase transition, and also sufficiently heavy Higgs eigenstates in the true vacuum, $m^t(T_r) > 2.3 T_r$, so that decays after the phase transition are suppressed by the low number density of Higgs bosons. No parameter sets satisfying the above were found.

The values of the sterile neutrino Yukawa coupling f to the Higgs singlet, presented in table I, are obtained by requiring that sterile neutrinos make up all the dark matter, where now the details of the two-component decay, the phase transition and the decoupling of degrees of freedom were taken into account. The numerical results are consistent with the estimate of eq. (21). The sterile neutrino mass $m_s = f \cdot \sigma_0$ is then set to be in the keV range.

VI. STERILE NEUTRINO PRODUCTION FROM OUT-OF-EQUILIBRIUM DECAYS

Finally, we address the possibility of S decoupling early from equilibrium and decaying into sterile neutrinos out of equilibrium. This is the case if $\alpha, \omega \approx 0$ and $\lambda_{HS} \approx 10^{-6}$. Then, only a second order, rather than a first order, phase transition occurs and the S decays happen in the broken phase.

The sterile neutrino population is again found from eq. (10), where now we need to determine the out-of-equilibrium concentration of S bosons.

The S boson number density N_S after decoupling, tak-

ing into account the annihilations of S bosons to SM particles, is given by [23]:

$$\frac{N_S(T)}{T^3} = \frac{N_S^{eq}(T_f)}{T_f^3} \frac{1}{2 - r_f/r} \quad (39)$$

If it were only for the $SS \rightarrow XX$ annihilations, the S boson abundance would decrease at $r \rightarrow \infty$ to just half of its equilibrium value at freeze-out. However, the decay of S particles to sterile neutrinos will result in an exponential damping of the S boson abundance. In addition, after H and S develop VEVs, S bosons will decay to SM fermions through the mixing with the SM Higgs. We can therefore ignore the $SS \rightarrow XX$ annihilations and consider only the $S \rightarrow N_a N_a$ and $S \rightarrow \bar{f} f$ decays to determine n_S after freeze out. The kinetic equation for S bosons is:

$$E \frac{\partial n_S}{\partial t} - H |\vec{p}|^2 \frac{\partial n_S}{\partial E} = -\frac{m^2 h^2}{8\pi} n_S, \quad (40)$$

where

$$h^2 \equiv \sum_a f_a^2 \left(1 - \frac{4f_a^2 \sigma^2}{m^2}\right) + \sum_f \lambda_f^2 \left(1 - \frac{4m_f^2}{m^2}\right) \left(\frac{\lambda_{HS}}{\max(\lambda_H, \lambda_S)}\right)^2 \quad (41)$$

takes into account the decay to all of the sterile neutrino species and SM fermions [45]. Here λ_f are the Yukawa couplings of the SM fermions to the Higgs doublet and $\frac{\lambda_{HS}}{\max(\lambda_H, \lambda_S)}$ is the mixing angle of the two Higgs mass eigenstates, at the limit $\lambda_{HS} \ll \lambda_H, \lambda_S$ and $\sigma \approx \eta$. Since S bosons live in the electroweak scale, the main fermion decay mode will be the $\bar{b} b$ channel. For $\lambda_{HS} \gtrsim 10^{-6}$, this dominates over the decays into keV sterile neutrinos. As we will see below, $\lambda_{HS} \approx 10^{-6}$ and $M_a \sim \text{keV}$ is a self-consistent set of parameters for producing a sufficient amount of sterile neutrinos to make up dark matter, through out-of-equilibrium decays of S bosons.

In terms of $r = m/T$ and $x_S = p_S/T$, one obtains:

$$\frac{\partial n_S}{\partial r} = -\frac{h^2 M_0}{8\pi m} \frac{r^2}{\sqrt{x_S^2 + r^2}} n_S. \quad (42)$$

This yields:

$$n_S(x_S, r) = \frac{1}{e^{\sqrt{x_S^2 + r^2}} - 1} \left(\frac{r + \sqrt{x_S^2 + r^2}}{r_f + \sqrt{x_S^2 + r_f^2}} \right)^{\Lambda x_S^2} \times e^{-\Lambda(r\sqrt{x_S^2 + r^2} - r_f\sqrt{x_S^2 + r_f^2})} \quad (43)$$

where we set $\Lambda = \frac{h^2 M_0}{16\pi m}$ and we took n_S to be the thermal equilibrium distribution function at $T = T_f$.

Using (42), eq. (10) can be partially integrated to give the sterile neutrino distribution function, produced by S

bosons decays after their freeze-out:

$$n^\Theta(x, r) = \frac{B}{x^2} \left[\int_{\left| \frac{r_f^2}{4x} - x \right|}^{\infty} x_S n_S(x_S, r_f) dx_S - \int_{r_f}^r \frac{r'}{2x} \left(\frac{r'^2}{4x} - x \right) n_S \left(\left| \frac{r'^2}{4x} - x \right|, r' \right) dr' - \int_{\left| \frac{r_f^2}{4x} - x \right|}^{\infty} x_S n_S(x_S, r) dx_S \right] \quad (44)$$

where we set $n^\Theta(x, r_f) = 0$ and

$$B \equiv \frac{f^2}{h^2} \quad (45)$$

is the branching ratio of $S \rightarrow N_1 N_1$ to all other decays, with N_1 being the lightest sterile neutrino. The last term in (44) vanishes at the limit $r \rightarrow \infty$, while the second term does not contribute to the total abundance, but only shifts the momentum distribution. The abundance of sterile neutrinos at any later time will be proportional to the amount of S bosons that have already decayed up to that time:

$$Y_s^\Theta(r) = B[Y_S(r_f) - Y_S(r)] \quad (46)$$

where

$$Y_S(r) = \frac{45}{4\pi^4 g_*} \int_0^\infty n_S(x_S, r) x_S^2 dx_S \quad (47)$$

is the S boson abundance, with $n_S(x_S, r)$ given by (43).

The production rate dY_s^Θ/dr peaks at some $r_{\text{prod}} = m/T_{\text{prod}}$. Since Λ determines how fast S bosons decay, r_{prod} depends on Λ but is effectively independent of r_f .

The amount of dark matter produced from the out of equilibrium decay of S bosons is:

$$\Omega_{\nu_s} \approx 0.2 \left(\frac{m_s}{3 \text{ keV}} \right) \left(\frac{Y_s^\Theta/B}{10^{-3}} \right) \left(\frac{B}{0.1} \right) \quad (48)$$

The variation of $Y_s^\Theta(\infty)/B$ vs r_f is shown in Fig.6. Early decoupling of S bosons $1 \lesssim r_f \lesssim 3$ implies $\lambda_{HS} \simeq 10^{-6}$ (cf. Fig. 1). The dominant decay mode is then $\bar{b}b$ pairs, with Yukawa coupling to the standard model Higgs $\lambda_b \simeq 2 \cdot 10^{-2}$. The branching ratio of S decays into an $m_s \simeq 3 \text{ keV}$ sterile neutrino, i.e. with $f = (1 - 5) \times 10^{-8}$, is $B \simeq 0.1 - 0.01$, since $\lambda_H, \lambda_S \sim 0.1 - 1$. The amount of sterile neutrinos produced by the out-of-equilibrium decays is then sufficient to constitute dark matter.

The average momentum at $r \rightarrow \infty$ of the sterile neutrino population produced through the out-of-equilibrium decays is

$$\frac{\langle p \rangle}{T} = \frac{\Lambda \int_{r_f}^\infty dr r^2 \int_0^\infty dx x^2 n_S(x, r)}{\int_0^\infty dx x^2 n_S(x, r_f)}. \quad (49)$$

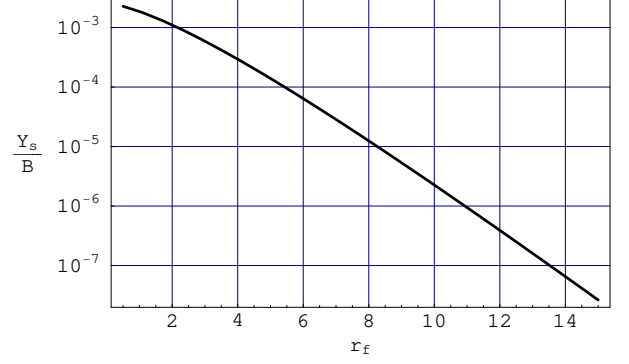


FIG. 6: The final sterile neutrino abundance $Y_s^\Theta(\infty)/B$ as a function of r_f .

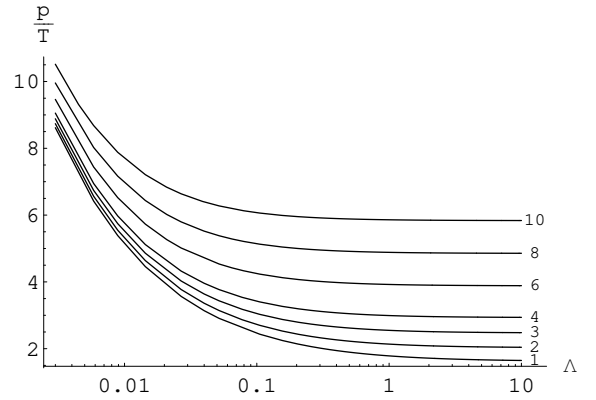


FIG. 7: Final average momentum $\langle p \rangle/T$ vs $\Lambda \propto h^2$, for various values of r_f , stated next to each curve. $\langle p \rangle/T$ is further redshifted by $\xi^{1/3} \approx 3.2$ with respect to the values presented in this graph.

The variation of $(\langle p \rangle/T)$ with Λ is shown in Fig. 7, for various values of r_f , where the redshifting factor $\xi^{1/3}$ (eq. (15)) has not yet been included. Then, for the set of parameters discussed above $\Lambda \approx 0.1$ and the production peaks at $r_{\text{prod}} \simeq 3$. Thus, the average momentum at the current temperature, for decoupling around $r_f \sim 1 - 2$, can be as low as (cf. Fig. 7):

$$\frac{\langle p \rangle}{T} \simeq \left(\frac{2.5}{\xi^{1/3}} \right)_{T \ll 1 \text{ MeV}} = 0.8. \quad (50)$$

Finally, we return to the in-equilibrium decay scenario. If $r_f > 3$, S bosons decay primarily while still in equilibrium. However, the amount of dark matter produced will be supplemented by any additional sterile neutrinos produced after S bosons come out of equilibrium. This again is given by eq. (48), where now both Y_s/B and B take lower values because of the increase in r_f and λ_{HS} . Thus, the amount of dark matter produced is determined only by a fraction of what was produced before the freeze-out, and our results from the previous section remain valid.

VII. BARYOGENESIS

The model under consideration and its minimal modifications offer at least two scenarios for generating the baryon asymmetry of the universe below the electroweak scale. One possibility is that the baryon asymmetry could arise from the low-scale leptogenesis if there are at least three sterile neutrinos below the electroweak scale, and if the two heavier ones are nearly degenerate in mass [30]. This scenario is different from the more commonly discussed thermal leptogenesis in that neutrino oscillations, not decays, are responsible for the change in the lepton number of the plasma. Active neutrinos (in equilibrium) can oscillate into the sterile neutrinos (out of equilibrium), and CP violation in the neutrino mass matrix could make the net lepton number of the out-of-equilibrium sterile neutrinos non-zero. The excess lepton number remaining in plasma is partially converted into the baryon number by sphalerons [30].

An alternative possibility exists if the phase transition is strongly first-order, which is quite likely in the model with the singlet, as discussed in Refs. [34, 35, 36]. In this case the standard electroweak baryogenesis [44] can take place in the course of this first-order phase transition. The model of eq. (3) can easily be modified to include a sufficient amount of CP violation: all that is required for a successful baryogenesis is to include the second Higgs doublet [35].

VIII. CONCLUSION

The inclusion of singlet fermions (right-handed neutrinos) in the Standard Model is the usual way to generate the observed neutrino masses [1]. In contrast with many other models, we assume that both Dirac and Majorana neutrino masses are generated via the Higgs mechanism [20]. The immediate advantage of this model is the possibility to produce dark matter, in the form of sterile neutrinos, which is cold enough to satisfy the bounds on the small-scale structure and the bounds from X-ray observations, while explaining the pulsar kicks at the same time [7]. The same sterile neutrinos can play an important role in the formation of the first stars [11]. We have considered different ways in which the dark-matter sterile neutrinos can be produced from the Higgs decays in the early universe. If the production from the Higgs decays dominates over the production by neutrino oscillations, the resulting dark matter population is colder than in the Dodelson-Widrow case for the same mass. The Higgs structure of the model has important implications for the collider physics and can be probed at the Large Hadron Collider and a Linear Collider [36, 43].

This work was supported in part by the DOE grant DE-FG03-91ER40662 and by the NASA ATP grant NAG 5-13399. A.K. appreciates hospitality of the Aspen Center for Physics.

-
- [1] P. Minkowski, Phys. Lett. **B67**, 421 (1977); M. Gell-Mann, P. Ramond, and R. Slansky, *Supergravity* (P. van Nieuwenhuizen et al. eds.), North Holland, Amsterdam, 1980; T. Yanagida, in *Proceedings of the Workshop on the Unified Theory and the Baryon Number in the Universe* (O. Sawada and A. Sugamoto, eds.), KEK, Tsukuba, Japan, 1979; S. L. Glashow, in *Proceedings of the 1979 Cargèse Summer Institute on Quarks and Leptons* (M. Lévy et al. eds.), Plenum Press, New York, 1980; R. N. Mohapatra and G. Senjanović, Phys. Rev. Lett. **44**, 912 (1980).
 - [2] S. Dodelson and L. M. Widrow, Phys. Rev. Lett. **72**, 17 (1994).
 - [3] K. Abazajian, G. M. Fuller and M. Patel, Phys. Rev. D **64**, 023501 (2001); A. D. Dolgov and S. H. Hansen, Astropart. Phys. **16**, 339 (2002); K. Abazajian, Phys. Rev. D **73**, 063506 (2006); T. Asaka, M. Laine and M. Shaposhnikov, JHEP **0606**, 053 (2006); JHEP **0701**, 091 (2007); D. Boyanovsky and C. M. Ho, JHEP **0707**, 030 (2007); Phys. Rev. D **76**, 085011 (2007); D. Boyanovsky, Phys. Rev. D **76**, 103514 (2007);
 - [4] X. d. Shi and G. M. Fuller, Phys. Rev. Lett. **82**, 2832 (1999).
 - [5] T. Asaka, S. Blanchet and M. Shaposhnikov, Phys. Lett. B **631**, 151 (2005); T. Asaka, M. Laine and M. Shaposhnikov, JHEP **0701**, 091 (2007); M. Shaposhnikov, Nucl. Phys. B **763**, 49 (2007); D. Gorbunov and M. Shaposhnikov, JHEP **0710**, 015 (2007);
 - [6] M. Shaposhnikov and I. Tkachev, Phys. Lett. B **639**, 414 (2006).
 - [7] A. Kusenko, Phys. Rev. Lett. **97**, 241301 (2006).
 - [8] K. Kadota, arXiv:0711.1570 [hep-ph].
 - [9] A. Kusenko and G. Segrè, Phys. Lett. B **396**, 197 (1997); A. Kusenko and G. Segre, Phys. Rev. D **59**, 061302 (1999); M. Barkovich, J. C. D'Olivo and R. Montemayor, Phys. Rev. D **70**, 043005 (2004); G. M. Fuller, A. Kusenko, I. Mocioiu, and S. Pascoli, Phys. Rev. D **68**, 103002 (2003); A. Kusenko, Int. J. Mod. Phys. D **13**, 2065 (2004).
 - [10] L. C. Loveridge, Phys. Rev. D **69**, 024008 (2004); C. L. Fryer, A. Kusenko, *Astrophys. J. Suppl.* **163**, 335 (2006); J. Hidaka and G. M. Fuller, Phys. Rev. D **74**, 125015 (2006); J. Hidaka and G. M. Fuller, Phys. Rev. D **76**, 083516 (2007).
 - [11] P. L. Biermann and A. Kusenko, Phys. Rev. Lett. **96**, 091301 (2006); M. Mapelli, A. Ferrara and E. Pierpaoli, Mon. Not. Roy. Astron. Soc. **369**, 1719 (2006); J. Stasielak, P. L. Biermann and A. Kusenko, *Astrophys. J.* **654**, 290 (2007); E. Ripamonti, M. Mapelli and A. Ferrara, Mon. Not. Roy. Astron. Soc. **375**, 1399 (2007); J. Stasielak, P. L. Biermann, A. Kusenko, arXiv:astro-ph/0701585; arXiv:0710.5431 [astro-ph].
 - [12] F. Munyaneza, P.L. Biermann, P. L., *Astron and Astrophys.*, **436**, 805 (2005); P. L. Biermann and F. Munyaneza, arXiv:astro-ph/0702173.
 - [13] K. Abazajian, G. M. Fuller and W. H. Tucker, *Astrophys. J.* **562**, 593 (2001); A. Boyarsky, A. Neronov, O. Ruchayskiy and M. Shaposhnikov, Mon. Not. Roy.

- Astron. Soc. **370**, 213 (2006); A. Boyarsky, A. Neronov, O. Ruchayskiy and M. Shaposhnikov, JETP Lett. **83**, 133 (2006); A. Boyarsky, A. Neronov, O. Ruchayskiy, M. Shaposhnikov and I. Tkachev, Phys. Rev. Lett. **97**, 261302 (2006); S. Riemer-Sorensen, S. H. Hansen and K. Pedersen, Astrophys. J. **644**, L33 (2006); K. Abazajian and S. M. Koushiappas, Phys. Rev. D **74**, 023527 (2006); C. R. Watson, J. F. Beacom, H. Yuksel and T. P. Walker, Phys. Rev. D **74**, 033009 (2006); K. N. Abazajian, M. Markevitch, S. M. Koushiappas and R. C. Hickox, Phys. Rev. D **75**, 063511 (2007); A. Boyarsky, J. Nevalainen and O. Ruchayskiy, Astron. Astrophys. **471**, 51 (2007); A. Boyarsky, O. Ruchayskiy and M. Markevitch, arXiv:astro-ph/0611168; S. Riemer-Sorensen, K. Pedersen, S. H. Hansen and H. Dahle, Phys. Rev. D **76**, 043524 (2007); A. Boyarsky, J. W. den Herder, A. Neronov and O. Ruchayskiy, Astropart. Phys. **28**, 303 (2007); H. Yuksel, J. F. Beacom and C. R. Watson, arXiv:0706.4084 [astro-ph]; A. Boyarsky, D. Iakubovskiy, O. Ruchayskiy and V. Savchenko, arXiv:0709.2301 [astro-ph].
- [14] M. Viel, et al., Phys. Rev. D **71**, 063534 (2005); U. Seljak, A. Makarov, P. McDonald and H. Trac, Phys. Rev. Lett. **97**, 191303 (2006) M. Viel, et al., A. Riotto, Phys. Rev. Lett. **97**, 071301 (2006). M. Viel, G. D. Becker, J. S. Bolton, M. G. Haehnelt, M. Rauch and W. L. W. Sargent, arXiv:0709.0131 [astro-ph].
- [15] A. Palazzo, D. Cumberbatch, A. Slosar and J. Silk, Phys. Rev. D **76**, 103511 (2007).
- [16] X. Hernandez, G. Gilmore, MNRAS **297**, 517 (1998); J. Sommer-Larsen, A. D. Dolgov, Astrophys. J. **551**, 608 (2001); F. Governato et al., Astrophys. J. **607**, 688 (2004); M. Fellhauer et al., Astrophys. J. **651**, 167 (2006); B. Allgood et al., MNRAS **367**, 1781 (2006); T. Goerdt et al., *ibid.*, **368**, 1073 (2006); G. Gilmore et al., Astrophys. J., **663**, 948 (2007); L. E. Strigari, J. S. Bullock, M. Kaplinghat, J. Diemand, M. Kuhlen and P. Madau, arXiv:0704.1817 [astro-ph]; R. F. G. Wyse, G. Gilmore, arXiv:0708.1492 [astro-ph];
- [17] G. Kauffmann, S. D. M. White and B. Guiderdoni, Mon. Not. Roy. Astron. Soc. **264**, 201 (1993); A. A. Klypin, A. V. Kravtsov, O. Valenzuela and F. Prada, Astrophys. J. **522**, 82 (1999); B. Moore, S. Ghigna, F. Governato, G. Lake, T. Quinn, J. Stadel and P. Tozzi, ApJ **524**, L19 (1999). B. Willman, F. Governato, J. Wadsley and T. Quinn, MNRAS, **355**, 159 (2004); P. Bode, J. P. Ostriker and N. Turok, Astrophys. J. **556**, 93 (2001). P. J. E. Peebles, ApJ, **557**, 495 (2001); J. J. Dalcanton and C. J. Hogan, Astrophys. J. **561**, 35 (2001); A. R. Zentner and J. S. Bullock, Phys. Rev. D **66**, 043003 (2002); J. D. Simon, A. D. Bolatto, A. Leroy and L. Blitz, Astrophys. J. **596**, 957 (2003); F. Governato et al., Astrophys. J. **607**, 688 (2004); G. Gentile, P. Salucci, U. Klein, D. Vergani and P. Kalberla, Mon. Not. Roy. Astron. Soc. **351**, 903 (2004); J. Kormendy, M. E. Cornell, D. L. Block, J. H. Knapen and E. L. Allard, Astrophys. J. **642**, 765 (2006); M. I. Wilkinson et al., arXiv:astro-ph/0602186; L. E. Strigari, J. S. Bullock, M. Kaplinghat, A. V. Kravtsov, O. Y. Gnedin, K. Abazajian and A. A. Klypin, Astrophys. J. **652**, 306 (2006); D. Boyanovsky, H. J. de Vega and N. Sanchez, arXiv:0710.5180 [astro-ph].
- [18] L. Gao and T. Theuns, Science **317**, 1527 (2007)
- [19] D. Boyanovsky, arXiv:0711.0470 [astro-ph].
- [20] Y. Chikashige, G. Gelmini, R. D. Peccei and M. Roncadelli, Phys. Lett. B **94**, 499 (1980). Y. Chikashige, R. N. Mohapatra and R. D. Peccei, Phys. Lett. B **98**, 265 (1981).
- [21] P. H. Frampton, S. L. Glashow and T. Yanagida, Phys. Lett. B **548**, 119 (2002).
- [22] T. Asaka, A. Kusenko and M. Shaposhnikov, Phys. Lett. B **638**, 401 (2006).
- [23] J. McDonald, Phys. Rev. D **50**, 3637 (1994).
- [24] K. Sigurdson and M. Kamionkowski, Phys. Rev. Lett. **92**, 171302 (2004); M. Kaplinghat, Phys. Rev. D **72**, 063510 (2005) J. A. R. Cembranos, J. L. Feng, A. Rajaraman and F. Takayama, Phys. Rev. Lett. **95**, 181301 (2005).
- [25] A. Kusenko, S. Pascoli and D. Semikoz, JHEP **0511**, 028 (2005). A. Y. Smirnov and R. Zukanovich Funchal, Phys. Rev. D **74**, 013001 (2006).
- [26] A. de Gouvêa, Phys. Rev. D **72**, 033005 (2005); A. de Gouvêa, J. Jenkins and N. Vasudevan, Phys. Rev. D **75**, 013003 (2007).
- [27] P. Candelas and S. Kalara, Nucl. Phys. B **298**, 357 (1988). D. Gepner, Nucl. Phys. B **311**, 191 (1988); W. Buchmuller, K. Hamaguchi, O. Lebedev, S. Ramos-Sanchez and M. Ratz, arXiv:hep-ph/0703078.
- [28] O. J. Eytan-Williams and S. F. King, JHEP **0506**, 040 (2005).
- [29] N. Arkani-Hamed, S. Dimopoulos, G. R. Dvali and J. March-Russell, Phys. Rev. D **65**, 024032 (2002); G. R. Dvali and A. Y. Smirnov, Nucl. Phys. B **563**, 63 (1999); E. A. Mirabelli and M. Schmaltz, Phys. Rev. D **61**, 113011 (2000).
- [30] E. K. Akhmedov, V. A. Rubakov and A. Y. Smirnov, Phys. Rev. Lett. **81**, 1359 (1998); T. Asaka and M. Shaposhnikov, Phys. Lett. B **620**, 17 (2005).
- [31] S. R. Coleman and E. Weinberg, Phys. Rev. D **7**, 1888 (1973).
- [32] L. Dolan and R. Jackiw, Phys. Rev. D **9**, 3320 (1974).
- [33] M. E. Carrington, Phys. Rev. D **45**, 2933 (1992).
- [34] K. Enqvist, K. Kainulainen and I. Vilja, Nucl. Phys. B **403**, 749 (1993); I. Vilja, Phys. Lett. B **324**, 197 (1994); S. W. Ham, Y. S. Jeong and S. K. Oh, J. Phys. G **31**, 857 (2005) A. Ahriche, Phys. Rev. D **75**, 083522 (2007)
- [35] J. McDonald, Phys. Lett. B **323**, 339 (1994).
- [36] S. Profumo, M. J. Ramsey-Musolf and G. Shaughnessy, JHEP **0708**, 010 (2007).
- [37] S. R. Coleman, Phys. Rev. D **15**, 2929 (1977) [Erratum-*ibid.* D **16**, 1248 (1977)].
- [38] A. D. Linde, Nucl. Phys. B **216**, 421 (1983) [Erratum-*ibid.* B **223**, 544 (1983)].
- [39] A. Kusenko, Phys. Lett. B **358**, 47 (1995) A. Kusenko, K. M. Lee and E. J. Weinberg, Phys. Rev. D **55**, 4903 (1997).
- [40] E. J. Weinberg and A. q. Wu, Phys. Rev. D **36**, 2474 (1987).
- [41] U. Sarid, Phys. Rev. D **58**, 085017 (1998) [arXiv:hep-ph/9804308].
- [42] G. Gelmini, S. Palomares-Ruiz and S. Pascoli, Phys. Rev. Lett. **93**, 081302 (2004).
- [43] T. Binoth and J. J. van der Bij, Z. Phys. C **75**, 17 (1997); A. Datta et al., Z. Phys. C **72**, 449 (1996). H. Davoudiasl, T. Han and H. E. Logan, Phys. Rev. D **71**, 115007 (2005); M. J. Strassler and K. M. Zurek, arXiv:hep-ph/0605193; D. O'Connell, M. J. Ramsey-Musolf and M. B. Wise, Phys. Rev. D **75**, 037701 (2007); V. Barger, P. Langacker and G. Shaughnessy, Phys. Rev. D **75**, 055013 (2007);

- V. Barger, P. Langacker, M. McCaskey, M. J. Ramsey-Musolf and G. Shaughnessy, arXiv:0706.4311 [hep-ph].
- [44] V. A. Kuzmin, V. A. Rubakov and M. E. Shaposhnikov, Phys. Lett. B **155**, 36 (1985).
- [45] We note in passing that sterile neutrinos with $\text{MeV} < M_a < M_S$ ($a \geq 2$), produced in the S decays, can de-

cay into three active neutrinos via mixing, in a tree-level process that involves Z exchange. Hence, we must take into account only the branching ratio of decay into the long-lived singlets with keV-scale masses.